MODELLING OF AN AIR-BASED BIPV/T WITH HEAT FINS IN ENERGYPLUS

Vuong E.*, Kamel R.S., Ekrami N., Leong W. H., Fung A. S.
*Author for correspondence
Department of Mechanical and Industrial Engineering,
Ryerson University,
Toronto, Ontario
Canada,
E-mail: e2vuong@ryerson.ca

ABSTRACT

A novel model of an air-based building integrated photovoltaic/thermal (BIPV/T) system with pin fins was developed in EnergyPlus V8.0 and was used to determine the improvement, in terms of thermal and electrical energy generation, over an un-finned BIPV/T system. The application of fins onto the internal channel surface will increase heat transfer from the PV panel to the air, which should increase thermal and electrical energy generation. The results from the model suggests that the finned BIPV/T system could produce a substantially greater amount of thermal energy than the un-finned system. However, the increase in electricity generation was minimal. Overall, the applications of fins in BIPV/T systems are effective modifications that will benefit any system that utilizes the thermal energy from the BIPV/T system. This finned BIPV/T model in EnergyPlus will allow users to apply these systems in the simulation of large-scale communities of buildings equipped with such systems.

INTRODUCTION

Installing fins and other thermally conductive material on Photovoltaic (PV) panels or Photovoltaic Thermal (PVT) collectors have been discussed to varying degrees of detail. According to Tripanagnostopoulos [1], the addition of fins are "practical modifications that enhance the heat transfer in the air channel". For finned PVTs, the heat transfer depends on the temperature gradient of the surface, geometry of the fin, thermal conductivity of fin and base surface, air flowrate and orientation of the array (angle of the PV panel) for low flowrates [2]. Fins have been installed on the rear surface of the PV panel, the opposite wall of the channel, and on both surfaces simultaneously [3,4]. For opaque BIPV/T systems (the PV backer material where the PV cells are laminated on is opaque), fins are best placed in direct contact with the PV (e.g. rear surface) in order to conduct the heat away from the PV cells [1]. However, this would prevent panels from being stacked, and will increase manfucturing and transportation costs. Tripanagnostopoulos [1] suggests that the installation of these fins on the opposite channel surface is less costly and much more simpler.

In these studies of PVTs and solar collectors with fins, few offer a Nusselt correlation intended for the heat transfer between the fins, base surface (which the fins are attached to) and airflow, either separately (e.g. correlation for the heat transfer between the fins and air alone, separate from the base) or as an array averaged value (combined heat transfer cofficient for the fins and base surface together). Naphon [5] developed a numerical model of an air solar collector and elected to use flat plate correlations that were applied by Ong [6]. Othman et al. [7] examined a double pass PVT with longitudinal fins and applied the same correlation that Ong [6] had employed. Karim and Hawlader [8] investigated flat plate solar collectors with fins and applied a flat plate Nusselt correlations developed by Sherwin [9] and Niles, Caxnegie, Pohl, and Cherne [10] for laminar and turbulent flow, respectively.

NOMENCLATURE

C_1	[-]	Constant for the combined base and fin Nusselt correlation
$h_{CONV,TOP}$	[kJ/hr·m^2·K]	Wind convective heat transfer coefficient
h_{FLUID}	[kJ/hr·m^2·K]	Convective heat transfer coefficient of the air within the air channel
$h_{FLUID,BOT}$	[kJ/hr·m^2·K]	Convective heat transfer coefficient of the air at the bottom surface of the channel
$h_{FLUID,TOP}$	[kJ/hr·m^2·K]	Convective heat transfer coefficient of the air at the combined base and fin surface
$h_{RAD\ 1,2}$	[kJ/hr·m^2·K]	Radiation heat transfer coefficient from the top to the bottom of the channel
$h_{RAD,TOP}$	[kJ/hr·m^2·K]	Radiation heat transfer coefficient from cover to the sky
n	[-]	Power constant for the combined base and fin Nusselt correlation
Nu_{Bottom}	[-]	Nusselt number at the bottom channel surface
$Nu_{Combined}$	[-]	Nusselt number at the combined surface
$q_U^{"}$	[kJ/hr·m^2]	Heat addition to the air within the channel
R_1	[hr·m^2·K/kJ]	Resistance of the PV glass cover
R_2	[hr·m^2·K/kJ]	Resistance of the PV backer material
R_3	[hr·m^2·K/kJ]	Resistance of the insulation of the roof
Re_D	[-]	Reynolds number based on the hydraulic diameter of the channel
Re_{FIN}	[-]	Reynolds number based on the fin length
S	[kJ/ hr]	Net thermal energy available from solar radiation, less the electricity generated
T_1	[°C]	Average temperature of the smooth top surface of the channel
T_2	[°C]	Average temperature of the smooth bottom surface of the channel
T_3	[°C]	Average temperature of the indoor wall temperature (given)
T_{AMB}	[°C]	Outdoor ambient temperature
T_{AVG}	[°C]	Average temperature of the combined base and fin surface
T_{COVER}	[°C]	Average temperature of the PV glass cover
T_{FLUID}	[°C]	Average air temperature in the channel
T_{PV}	[°C]	Average PV cell temperature
T_{SKY}	[°C]	Sky temperature
Z_1	[-]	Ratio of the finned heat transfer area to the area of the PV panel

There were many experimental studies on the performance of circular pin fins, with the end goal application for turbine blade cooling. In these cases, long fins (defined as having a fin length to diameter ratio greater than 4 [11]) are not used; instead, short fins are favoured. Circular pin fins were attached to a horizontal base plate with adhesive [12] or with fasteners [13, 2]. In a study, fin spacing, channel height, array angle (relative to the entering air) and fin diameter were examined by preparing a 0.2 m by 0.2 m base plate with circular fins [14]. The finned plate of the assembly, which formed a channel, was heated and air flow passed over it, with thermocouples measuring the temperature of the system. Maudgal and Sunderland [14] later presented Nusselt correlations, for Reynolds numbers (based on the fin length) of 2500 to 5100. Similar experimental setups, with different fin and channel sizes and different air flowrates were also used by Tahat et al. [2] although Maudgal and Sunderland [14] used the napthalene sublimation technique instead of applying thermocouples in their experiment.

Air source heat pumps (ASHPs) have the potential to eliminate the use of natural gas for residential heating [15]. However, their efficiency drops tremendously in frigid Canadian winters. This disadvantage can be alleviated by coupling the ASHP with a building integrated photovoltaic/thermal (BIPV/T) system. BIPV/T systems are photovoltaic (PV) panels fully integrated into the building envelope with a fluid circulating behind it, in order to extract thermal energy while the PV generates electricity. By using air as the circulating fluid, a BIPV/T system can provide a source of preheated air for ASHPs. This would allow ASHPs to operate at a higher coefficient of performance (COP), since it does not have to extract heat from the colder ambient air.

ASHPs require high air temperature in order to increase its COP; however, it also requires a large amount of thermal energy to meet heating demands. Although BIPV/T systems can provide preheated air for an ASHP, there is a challenge in providing air at a relatively high temperature and satisfying heating demands. This occurs because in order to collect enough thermal energy, the flowrate through the BIPV/T system must increase. However, this will also result in a lower BIPV/T outlet air temperature. Thus, attempting to increase the outlet air temperature (by lowering the flowrate) will result in less thermal energy, and attempting to increase thermal energy (by increasing the flowrate) will result in a lower outlet air temperature.

This problem can be alleviated by installing heat fins onto the top surface of the channel in a BIPV/T system. The fins will increase the heat transfer area and promote turbulent flow, thus augmenting heat transfer within the channel. As a result, for the same flowrate, a finned BIPV/T system should provide more thermal energy at a higher outlet temperature than an un-finned BIPV/T system. This paper details a preliminary analysis of the potential benefit of adding fins to the top channel surface of a BIPV/T system (rear surface of the PV panel), with respect to thermal and electrical power generation. Based on a previously developed BIPV/T model in EnergyPlus (a building energy simulation program) [16], a numerical finned BIPV/T model was developed using a fin Nusselt correlation and was used as a simulation tool in this analysis.

UN-FINNED AND FINNED BIPV/T MODEL

EnergyPlus is a building simulation program developed by the US Department of Energy. For this analysis, a finned BIPV/T model was written in FORTRAN and implemented into EnergyPlus. The model was based on the BIPV/T model (Type 298 in TRNSYS), which was developed by Kamel and Fung [15], and the Nusselt correlation for fins in a channel developed by [14] was incorporated.

Schematics of the un-finned and finned BIPV/T system are shown in Figures 1 and 2, respectively.

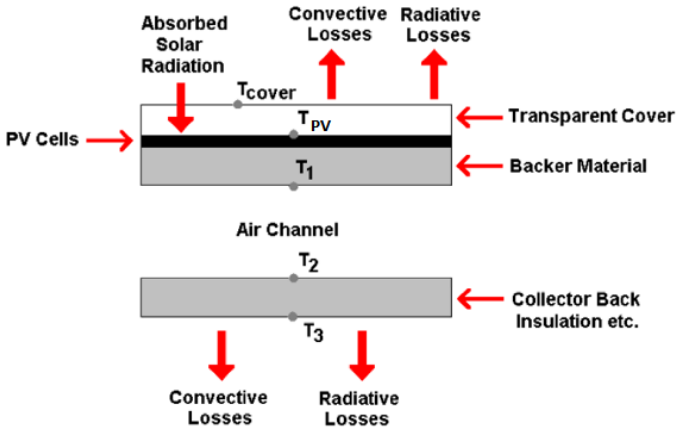

Figure 1 Un-finned BIPV/T [17]

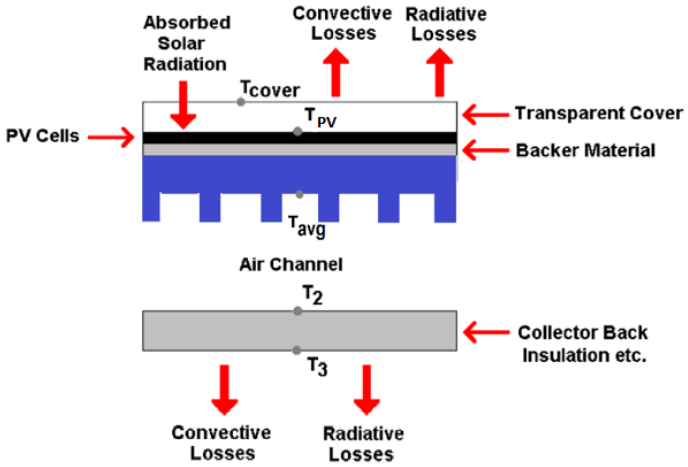

Figure 2 Finned BIPV/T (modified from Figure 1)

Equations (1) to (5) are the steady-state energy balances of the un-finned EnergyPlus model, which were obtained from the TRNSYS 17 manual [17]; note that there is a single common heat transfer coefficient for both channel's top and bottom surfaces (temperature nodes , T_1 and T_2, respectively).

$$\frac{T_{PV}-T_{COVER}}{R_1} = h_{CONV,TOP}\,(T_{COVER} - T_{AMB}) + h_{RAD,TOP}(T_{COVER} - T_{SKY}) \quad (1)$$

$$S = \frac{T_{PV}-T_{COVER}}{R_1} + \frac{T_{PV}-T_1}{R_2} \quad (2)$$

$$\frac{T_{PV}-T_1}{R_2} = h_{FLUID}(T_1 - T_{FLUID}) + h_{RAD\ 1,2}(T_1 - T_2) \quad (3)$$

$$q''_U = h_{FLUID}(T_1 - T_{FLUID}) - h_{FLUID}(T_{FLUID} - T_2) \quad (4)$$

$$\frac{T_2-T_3}{R_3} = h_{FLUID}(T_{FLUID} - T_2) + h_{RAD\ 1,2}(T_1 - T_2) \quad (5)$$

Equations (6) to (10) are the steady-state energy balances of the finned BIPV/T model in Figure 2. As mentioned previously, the finned model is based on the un-finned model with modifications.

$$\frac{T_{PV}-T_{COVER}}{R_1} = h_{CONV,TOP}\,(T_{COVER} - T_{AMB}) + h_{RAD,TOP}(T_{COVER} - T_{SKY}) \quad (6)$$

$$S = \frac{T_{PV}-T_{COVER}}{R_1} + \frac{T_{PV}-T_{AVG}}{R_2} \quad (7)$$

$$\frac{T_{PV}-T_{AVG}}{R_2} = Z_1\, h_{FLUID,TOP}(T_{AVG} - T_{FLUID}) + h_{RAD\ 1,2}(T_{AVG} - T_2) \quad (8)$$

$$q''_U = Z_1 h_{FLUID,TOP}(T_{AVG} - T_{FLUID}) - h_{FLUID,BOT}\,(T_{FLUID} - T_2) \quad (9)$$

$$\frac{T_2-T_3}{R_3} = h_{FLUID,BOT}(T_{FLUID} - T_2) + h_{RAD1,2}(T_{AVG} - T_2) \quad (10)$$

T_1 in the un-finned model has been replaced by T_{AVG} in the finned model, which represents the average temperature of the combined base-fin surface (the entire purple section in Figure 2). It is assumed that the combined base-fin surface has negligible thermal resistance. Furthermore, in this finned model, there are two convective heat transfer coefficients, one for the combined base-fin surface and a second one for the bottom channel surface. The combined base-fin heat transfer coefficient, $h_{FLUID,TOP}$, is a fin array averaged coefficient that is determined using the Nusselt correlation for an array of circular pin fins in a rectangular duct. The top Nusselt correlation is presented in Equation (11) and was developed by Maudgal and Sunderland [14].

$$Nu_{Combined} = C_1\,(Re_{FIN})^n \quad (11)$$

C_1 and n are constants that are dependent on the diameter to spacing ratio and the fin tip clearance. The bottom heat transfer coefficient, $h_{FLUID,BOT}$, is the heat transfer coefficient of the bottom surface (with temperature node T_2), and is estimated using the same correlation as used in Type 298 [15]; it is assumed that the fin lengths are not long enough to disrupt the boundary layer of the bottom surface. This bottom coefficient is estimated using the following correlation,

$$Nu_{Bottom} = 0.0158\,{Re_D}^{0.8} \quad (11)$$

The variable Z_1 is the ratio of the finned heat transfer area to the area of the PV panel (since area of the combined base-fin surface is greater than the area of the PV, $Z_1 > 1$).

SIMULATION PARAMETERS

Both of the un-finned and finned BIPV/T systems consisted of five PV panels (1.2 m^2 with 16% efficiency at standard rated conditions), forming one row of a BIPV/T system. In these systems, ambient air is drawn through the first panel and exits the system after the fifth panel, at 0.1 kg/s. Only one row was simulated because in a roof-façade BIPV/T system the performance of all the adjacent rows of PV panels would be similar, due to uniform solar radiation over the roof. In the model, a one-dimensional heat flow is assumed. The circular fins in the finned-BIPV/T system were of 0.03 m in diameter, arranged in an in-line pattern spaced between fin centers at 0.055 m in the axial and transverse directions, and were 0.0381 m in length. The finned array area was 0.73 m^2. The study was based on the winter weather in Toronto, Canada, a cold climate region.

TRENDS AND RESULTS

Using the finned BIPV/T model in EnergyPlus to simulate a finned BIPV/T system, the results for all the temperature, thermal, and electrical outputs were obtained and compared with that of an un-finned BIPV/T system. It was found that the finned BIPV/T system produced much more thermal energy, due to higher heat transfer rates.

In BIPV/T systems, the solar energy is absorbed by the PV cells, increasing its temperature. In an un-finned BIPV/T system, the heat is conducted to the upper surface of the air channel and then transferred to the moving air. Similarly, in the finned system, the heat is transmitted to the combined base-fin surface, where it is convected to the air. In addition to convective heat transfer between the upper surface or combined base-fin surface and the air, the heat is also transferred via radiation to the opposite surface of the channel.

Due to the presence of the fins, the convective heat transfer was augmented by an increased heat transfer area and the higher turbulent flow regime. Hence, in the finned system, the combined base-fin surface's temperature is lower than the un-finned system's upper surface. This is shown in Figure 3, which depicts the upper un-finned and combined base-fin surfaces' temperatures of the final panel (fifth panel) of both BIPV/T systems throughout a cold and sunny day. There is a larger difference between the two temperatures during the hours of 10 am to 4 pm because there is a larger amount of solar radiation during the day; hence, the fins are able to increase the heat transfer rate. However, in the early morning and late afternoon hours, the amount of solar radiation is low; hence, the finned system operates at a level close to that of the un-finned system.

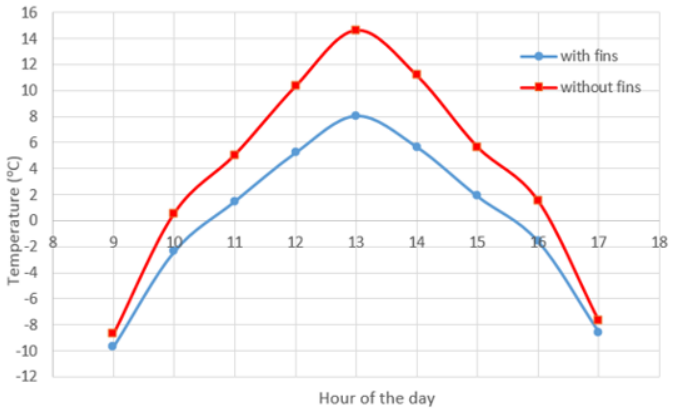

Figure 3 Fifth PV panel's upper un-finned surface and combined base-fin surface

This lower combined base-fin surface temperature also resulted in a lower PV temperature, as shown in Figure 4, which depicts the averaged PV cell temperature of each of the five panels at 1 pm. The smaller difference between the two systems' PV temperatures, as compared to their two surface temperatures in Figure 3, is due to the resistance of the backer material of the PV panel.

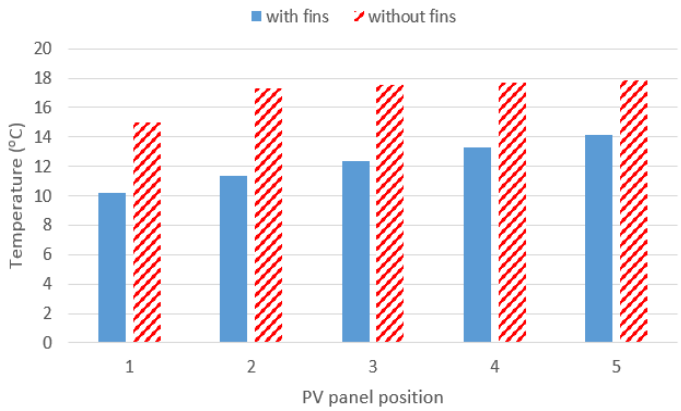

Figure 4 PV panel temperatures at 1 pm

Due to the lower temperatures of these two layers, more heat was transferred to the air and, hence, the outlet air temperature of the finned BIPV/T system is greater than the un-finned system's, which is depicted in Figure 5. The outdoor ambient temperature is also shown in order to provide a reference as to the amount of temperature gain possible with BIPV/T systems. At 1 pm, with the greatest amount of solar radiation, the un-finned BIPV/T system alone could heat -10 ºC ambient air up to approximately -3.5 ºC, a 6.5 ºC increase. On the other hand, for the same flowrate, the finned system could heat the same air up to almost 2 ºC, a 12 ºC increase. Even though the ambient temperature remained constant from 11 am to 3 pm, the outlet temperature increased until 1 pm because more solar radiation was available.

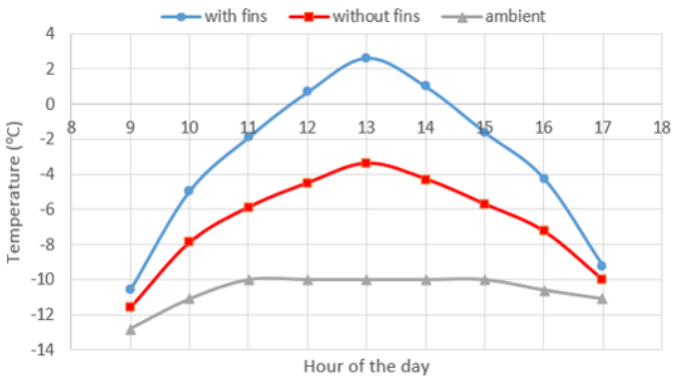

Figure 5 Hourly BIPV/T system outlet air temperature

The increased outlet air temperature resulted in an increased in thermal energy generation since the two BIPV/T systems had the same air flowrate. In Figure 6, the thermal output of the two BIPV/T systems are presented. Over the entire day, the finned system produced 24,000 kJ (6.67 kWh) of thermal energy, compared to 12,700 kJ (3.53 kWh) of thermal energy produced by the un-finned system. That is, if the heating demand of a house was 12,700 kJ (3.53 kWh) at that particular hour, the finned system could provide that amount of energy at approximately half the flowrate of an un-finned BIPV/T system. Although BIPV/T systems are less efficient at lower ambient temperatures and the finned BIPV/T system may not always produce twice the thermal energy of the un-finned system, these results demonstrates that fins are feasible modifications to the BIPV/T systems that are intended to provide more thermal energy.

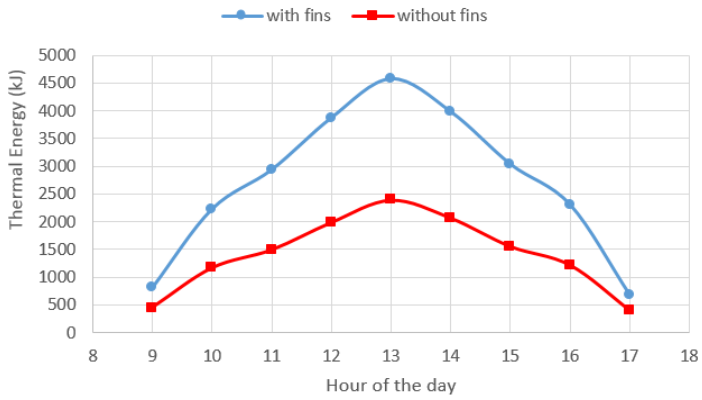

Figure 6 Hourly BIPV/T thermal energy production

The electrical energy produced by the two BIPV/T systems are presented in Figure 7. Although the finned system managed to extract more thermal energy from the PV cells and reduced its temperatures, as shown in Figure 4, it did not generate that much more electrical energy than the un-finned system. During this day, the finned system generated 18,335 kJ (5.09 kWh) of electricity, while the un-finned system generated 18,035 kJ (5.01 kWh) of electricity. This is due to the property of the PV panel,

where the change in efficiency per degree Celsius change in the PV temperature is small.

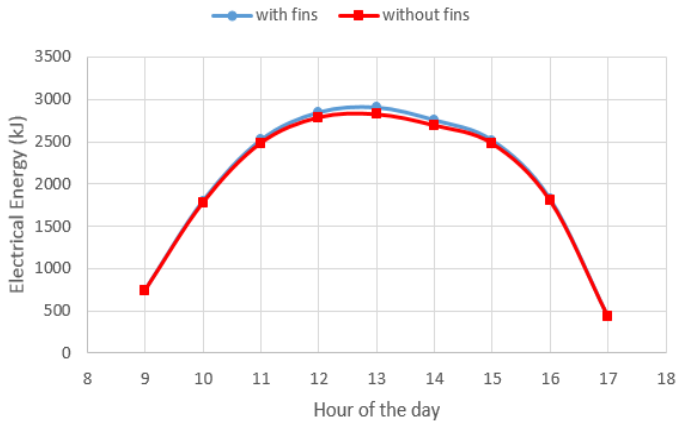

Figure 7 Hourly BIPV/T electricity production

According to [15], decreasing the PV temperature would increase electrical efficiency of the cells. Therefore, by further decreasing the temperature, the electrical production should increase. However, the increased PV cell efficiency due to the several degrees of Celsius difference, even in the last panel (the warmest of the five), did not increase the electricity generated by a significant amount.

CONCLUSION

A finned BIPV/T model was developed in EnergyPlus and used to examine the potential increase in thermal and electrical output of an opaque BIPV/T system, in order to quantify the benefit of finned BIPV/T systems. The results show that the finned BIPV/T system approximately doubled the un-finned system's thermal output. This would solve the challenge that BIPV/T systems have, i.e., providing a large amount of thermal energy with relatively higher outlet air temperature. However, the results show that there was little benefit to the electrical output of the PV system. Hence, the finned BIPV/T systems are beneficial in increasing thermal output; but in part due to the property of the PV panel, they have little effect on increasing electricity generation. These results suggest that fins are feasible modifications that can be included in the BIPV/T systems that are coupled with ASHP.

ACKNOWLEDGEMENT

The authors would like to acknowledge the funding and support from the NSERC Discovery Grant, Smart Net-Zero Energy Building Research Network (SNZBRN), TRCA, and MITACS.

REFERENCES

[1] Tripanagnostopoulos, Y. (2007). Aspects and improvements of hybrid photovoltaic/thermal solar energy systems. *Solar Energy, 81*(9), 1117-1131.

[2] Tahat, M., Kodah, Z. H., Jarrah, B. A., & Probert, S. D. (2000). Heat transfers from pin-fin arrays experiencing forced convection. *Applied Energy, 67*(4), 416-442.

[3] Garg, H. P., & Datta, G. (1989). Performance studies on a finned-air heater. *Energy, 14*(2), 87-82.

[4] Garg, H. P., Jha, R., & Datta, G. C. (1991). Theoretical analysis on a new finned type solar air heater. *Energy, 16*, 1231-1238.

[5] Naphon, P. (2005). On the performance and entropy generation of double-pass solar air heater with longitudinal fins. *Renewable Energy, 30*(9), 1345-1357.

[6] Ong, K. S. (1995). Thermal performance of solar air heaters: Mathematical model and solution procedure. Solar Energy, 55(2), 93-109.

[7] Othman, M. Y., Yatim, B., Sopian, K., & Abu Bakar, M. N. (2005). Performance analysis of a double-pass photovoltaic/ thermal (PV/T) solar collector with CPC and fins. *Renewable Energy, 30(13)*, 2005-2017.

[8] Karim, M. A., & Hawlader, M. N. (2006). Performance investigation of flat plate, v-corrugated and finned air collectors. *Energy*(4), 452-470.

[9] Sherwin, K. (1985). The heat transfer of plate fin and circular tube geometry. Third Australian Conference on Heat and Mass Transfer (pp. 441-447). Melbourne: Third Australian Conference on Heat and Mass Transfer.

[10] Niles, P., Caxnegie, E. J., Pohl, J. G., & Cherne, J. M. (1979). Design and performance of an air collector for industrial crop drying. Solar Energy, 20, 19-28.

[11] Lyall, M. E., Thrift, A. A., Thole, K. A., & Kohli, A. (2011). Heat Transfer From Low Aspect Ratio Pin Fins. *Journal of Turbomachinery, 133*(1), 011001-011001-10.

[12] Kotcioglu, I., Caliskan, S., & Baskaya, S. (2011). Experimental study on the heat transfer and pressure drop of cross-flow heat exchangers with different pin-fin arrays. *Heat Mass Transfer, 47*(9), 1133-1142.

[13] Sparrow, E. M., & Ramsey, J. W. (1978). Heat Transfer and Pressure Drop for a Staggered Wall-Attached Array of Cylinders with Tip Clearance. *International Journal of Heat Mass Transfer, 21*, 1369-1377.

[14] Maudgal, V. K., & Sunderland, J. E. (1997). An experimental study of forced convection heat transfer from in-line pin fin arrays. *Thirteenth Annual IEEE Semiconductor Thermal Measurement and Management Symposium*, (pp. 149-157).

[15] Kamel, R. S., & Fung, A. S. (2014). Modeling, simulation and feasibility analysis of residential BIPV/T+ASHP system in cold climate—Canada. *Energy and Buildings*, 82, 758-770.

[16] Vuong E., Kamel, R. S., & Fung, A. S. (2015) Modelling and Simulation of BIPV/T in EnergyPlus and TRNSYS. *Energy Procedia*, 78, 1883-1888.

[17] TRNSYS. (2012). *TRNSYS 17 Reference Manual.* Madison, WI: Solar Energy Lab, Univ. of Wisconsin-Madison.